Cell Stem Cell
Article

The Epidermis Comprises Autonomous Compartments Maintained by Distinct Stem Cell Populations

Mahalia E. Page,[1,2] Patrick Lombard,[1,3] Felicia Ng,[1,3] Berthold Göttgens,[1,3] and Kim B. Jensen[1,2,4,*]
[1]Wellcome Trust - Medical Research Council Cambridge Stem Cell Institute, Tennis Court Road, CB2 1QR Cambridge, UK
[2]Department of Oncology, University of Cambridge, CB2 0QQ Cambridge, UK
[3]Department of Haematology, Cambridge Institute for Medical Research, CB2 0XY Cambridge, UK
[4]Biotech Research and Innovation Center, University of Copenhagen, 2200 Copenhagen N, Denmark
*Correspondence: kim.jensen@bric.ku.dk
http://dx.doi.org/10.1016/j.stem.2013.07.010

SUMMARY

The complex anatomy of the epidermis contains multiple adult stem cell populations, but the extent to which they functionally overlap during homeostasis, wound healing, and tumor initiation remains poorly defined. Here, we demonstrate that Lrig1^{+ve} cells are highly proliferative epidermal stem cells. Long-term clonal analysis reveals that Lrig1^{+ve} cells maintain the upper pilosebaceous unit, containing the infundibulum and sebaceous gland as independent compartments, but contribute to neither the hair follicle nor the interfollicular epidermis, which are maintained by distinct stem cell populations. In contrast, upon wounding, stem cell progeny from multiple compartments acquire lineage plasticity and make permanent contributions to regenerating tissue. We further show that oncogene activation in Lrig1^{+ve} cells drives hyperplasia but requires auxiliary stimuli for tumor formation. In summary, our data demonstrate that epidermal stem cells are lineage restricted during homeostasis and suggest that compartmentalization may constitute a conserved mechanism underlying epithelial tissue maintenance.

INTRODUCTION

A common feature of epithelial tissues such as the epidermis, small intestine, lung, and mammary gland is the coexistence of multiple distinct adult stem cell populations (Van Keymeulen and Blanpain, 2012; Rock and Hogan, 2011). In some of these tissues such as the epidermis and intestine, the stem cell heterogeneity is well characterized, but its functional consequences in terms of tissue maintenance and response to injury or insult remain poorly understood (Barker et al., 2012; Jaks et al., 2010). In other tissues like the mammary gland and prostate, distinct stem cell populations are responsible for maintaining the luminal and basal compartments independently during homeostasis (Van Keymeulen et al., 2011; Ousset et al., 2012; Choi et al., 2012). It is possible that the same lineage restrictions occur in the epidermis.

The epidermis forms the outer protective layer of the skin and comprises the interfollicular epidermis (IFE) with associated adnexal structures such as the pilosebaceous unit. The pilosebaceous unit includes the hair follicle (HF) and the sebaceous gland (SG) and is attached to the IFE via the infundibulum. Here, an enormous cellular complexity provides the basis for its long-term replenishment. The IFE is maintained by a combination of long-lived stem cells (SCs) and committed progenitors (Clayton et al., 2007; Mascré et al., 2012). SCs in the lower permanent bulge region of the pilosebaceous unit (hair follicle stem cells, HF-SCs) are responsible for hair regrowth and express markers such as Gli1, Lgr5, keratin 15, keratin 19, and CD34 (Jaks et al., 2010). The isthmus, which forms the lower portion of the upper pilosebaceous unit, contains multiple partly overlapping populations marked by the expression of Lgr6, Plet1/Mts24, and Lrig1 (Jensen et al., 2009; Nijhof et al., 2006; Snippert et al., 2010). Adjacent to the isthmus at the junctional zone (JZ) region is the SG, which forms during development from an early population of Lrig1 expressing precursor cells and is subsequently maintained by Blimp1-expressing cells (Jensen et al., 2009; Frances and Niemann, 2012; Horsley et al., 2006). The relationship between the individual compartments in the epidermis is still an open question.

Fate mapping based on inducible-marker expression is the preferred method for delineating cell behavior in vivo (Alcolea and Jones, 2013; Van Keymeulen and Blanpain, 2012). This technique has formed the basis for understanding how complex tissues are maintained. With the use of lineage tracing, it has been possible to identify stem cells that contribute to most epidermal components, but it has so far been impossible to determine whether the epidermis is maintained in a hierarchal manner or as independent compartments governed by higher-order structural arrangements. Moreover, the population responsible for the maintenance of the uppermost part of the pilosebaceous unit, the infundibulum, remains elusive. HF-SCs have been reported to replenish the other epidermal SC niches and therefore act as multipotent master SCs at the top of a cellular hierarchy (Morris et al., 2004; Petersson et al., 2011). Similarly, progeny of multipotent Lgr6-expressing SCs in the isthmus are detected both in the SG and IFE (Snippert et al.,

2010). In sharp contrast, additional studies have shown that the pilosebaceous unit including the infundibulum is maintained independently of the IFE in the absence of wounding (Ghazizadeh and Taichman, 2001; Levy et al., 2005; Nowak et al., 2008). The extent of contribution from each epidermal SC population to the different epidermal lineages and the overall arrangement of tissue maintenance remain unresolved.

Genetic perturbation and changes in the local microenvironment affect cell behavior and the lineage commitment of epidermal SCs (Owens and Watt, 2003). This is evident from the role of epidermal SCs upon injury (Plikus et al., 2012). Recent evidence from fate-mapping studies demonstrates that otherwise slowly proliferating SCs are the cells within the IFE that make the major contribution to wound repair (Mascré et al., 2012). SCs from the pilosebaceous unit are also mobilized to participate in repair of the IFE (Ito et al., 2005). However, once in the IFE, the cellular origin within the pilosebaceous unit appears to influence the capacity to be maintained long term (Jaks et al., 2010). It remains to be understood whether certain SC progeny are selectively retained in the wound or whether loss of SC progeny from the wound site after healing is a stochastic process.

Lrig1 is one of multiple markers associated with SCs in the upper pilosebaceous unit (Jaks et al., 2010; Jensen et al., 2009), as well as in other tissues (Wong et al., 2012; Lu et al., 2013). In the epidermis, these cells are capable of contributing to all epidermal lineages in skin-reconstitution assays (Jensen et al., 2009); however, their exact lineage potential during normal homeostasis and the functional relevance of the observed epidermal SC heterogeneity remain unresolved. In this study we address SC heterogeneity within the epidermis with the aim to (1) determine whether SC populations have distinct features; (2) assess the hierarchal relationship between SCs during steady-state homeostasis; and (3) investigate how SC identity affects cell behavior upon tissue perturbation.

RESULTS

Stem Cell Heterogeneity in the Pilosebaceous Unit

In order to investigate the properties and physical relationship of distinct SC populations in epidermal homeostasis, we utilize a mouse model with EGFP-ires-CreERT2 inserted at the translational start site in exon 1 of the Lrig1 locus (Lrig1 knockin [KI]; Figure S1A available online). This mouse model, in combination with validated antibodies, enables us to assess the physical overlap of SCs populations in the pilosebaceous unit (Figure 1A). Importantly, the Lrig1 KI model faithfully reproduces the expression of endogenous Lrig1 protein (Figures 1B–1D; Figures S2A–S2C).

During the resting (telogen) phase of the HF cycle, Lrig1 is expressed by cells in the upper isthmus and SG distinct from CD34^{+ve} HF-SCs (Figure 1E). Lrig1-EGFP^{+ve} cells express reduced levels of Sca1, a protein expressed highly by cells in the IFE (Figure 1F; Jensen et al., 2008). During the growth (anagen) phase of the hair cycle, Lrig1 expression extends into the outer root sheath and hair germ (Figure 1G; Jensen et al., 2009). Similar to the intestinal tract, Lrig1 is here coexpressed with Lgr5 (Wong et al., 2012). In order to restrict our analysis to Lrig1-expressing cells in the upper pilosebaceous unit, all subsequent experiments have been carried out in telogen back skin. This analysis is supported by data from tail epidermis, where the hair cycle is asynchronous.

The upper pilosebaceous unit contains multiple SC populations marked by Lrig1, Plet-1/MTS24, Lgr6, and Blimp1 expression (Horsley et al., 2006; Nijhof et al., 2006; Jensen et al., 2009; Snippert et al., 2010). By assessing the individual markers, we show that Lrig1 and Plet1/MTS24 are expressed in the same location (Figure 1H). The expression of Lgr6 is more widespread and can be detected in the HF-SC niche, in the IFE, and in the SG in addition to the reported expression in the isthmus (Figure 1I; Figures S1C and S1D; Snippert et al., 2010). Here, Lrig1 and Lgr6-EGFP define partly overlapping domains of cells. Similar coexpression is observed in the SG (Figure 1I). These Lrig1-EGFP^{+ve} cells in the basal layer of the SG are distinct from Blimp1^{+ve} cells, which are suprabasal and have a pronounced differentiated morphology as previously reported (Figure 1J; Cottle et al., 2013). The pattern of marker expression is further substantiated by coexpression of *Lrig1* and *Plet1/MTS24* at the RNA level (Figure 1K).

We conclude that Lrig1 and Plet-1/MTS24 are expressed by cells in the same location in the upper isthmus, and that these cells are distinct from cells expressing Blimp1 in the SG. In addition, Lgr6 expression is not restricted to the isthmus as previously reported (Snippert et al., 2010), given that scattered Lgr6-EGFP^{+ve} cells are present throughout the entire epithelium.

Lrig1 Marks a Population of Highly Proliferative Epidermal Cells

In order to assess whether Lrig1-expressing cells are molecularly distinct from HF-SCs and basal cells in the epidermis, Lrig1-EGFP^{+ve} cells, CD34^{+ve} HF-SCs, and ItgA6^{+ve}Lrig1^{-ve}CD34^{-ve} cells, which primarily represent basal undifferentiated IFE cells, were isolated for transcriptional analysis (Figures 2A and 2B; Table S1). Principal component analysis identifies the three different subsets of cells as distinct (Figure 2C). Hierarchal clustering of differentially expressed genes shows that Lrig1-EGFP^{+ve} cells are more related to IFE cells than to the HF-SC (Figure 2D). There is, however, a subset of 92 probe sets associated with 58 annotated genes, which are shared between the two SC populations including markers previously identified as HF-SC markers (Figures 2E and S1G; Table S2). A set of 73 probes corresponding to 49 annotated genes is specifically associated with the Lrig1^{+ve} compartment. Interestingly, these include *Ccl2* and *Ccl7*, which are two inflammatory cytokines previously associated with the stressful environment in the upper pilosebaceous unit (Nagao et al., 2012).

Gene Ontology (GO) analysis of Lrig1-expressing cells versus IFE cells reflects the functionality of the two populations. Here, cells in the IFE express genes associated with lipid metabolism, which is integral to barrier formation, whereas Lrig1^{+ve} cells have elevated expression of genes associated with receptor protein kinase signaling, cell adhesion, and migration, as well as various development pathways (Table S3). In line with the clustering analysis and the individual comparison of the three populations (Figures 2D and 2E), a vast number of genes are enriched in the CD34-expressing compartment. The majority are associated with development and morphogenetic and differentiation pathways (Table S3). Comparison of Lrig1^{+ve} with CD34-expressing cells reveals a strong enrichment for genes associated with proliferation in the Lrig1^{+ve} compartment. Moreover, Lrig1-EGFP^{+ve}

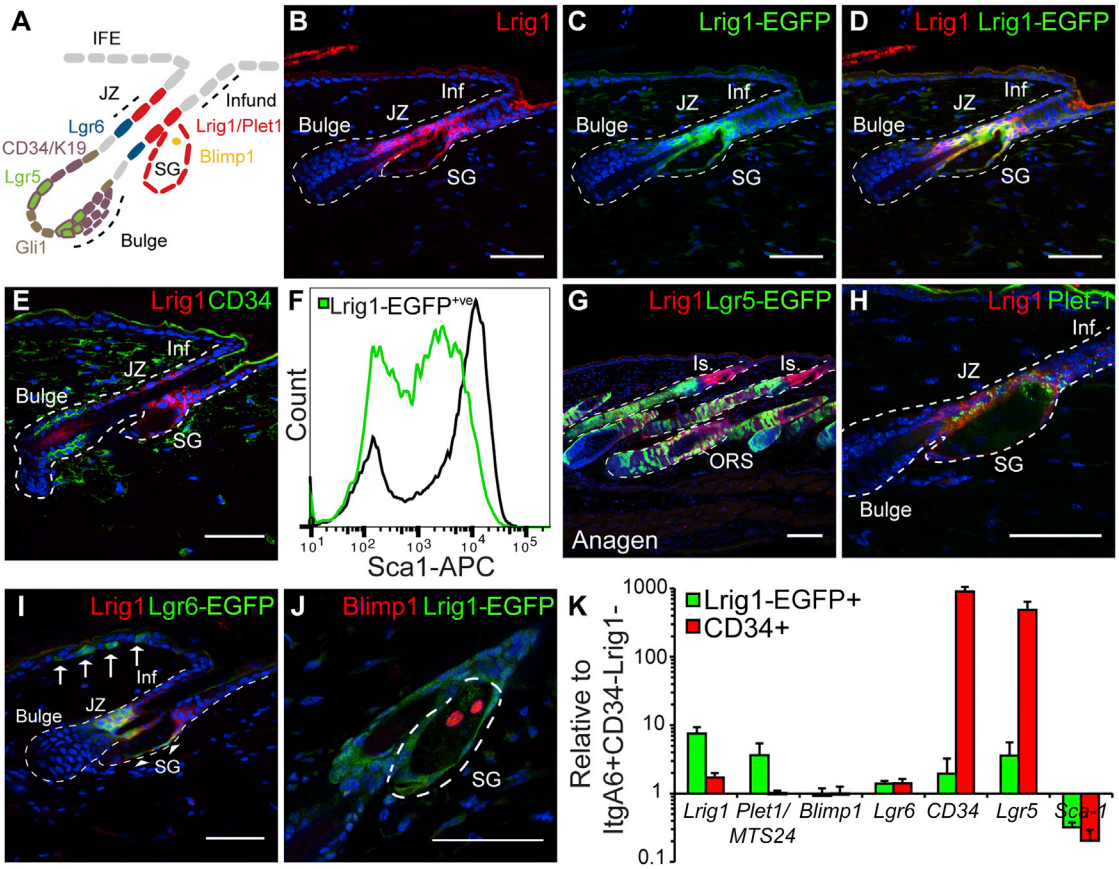

Figure 1. Characterization of SC Heterogeneity in the Epidermis

(A) Schematic diagram of SC populations in the mouse pilosebaceous unit. Infund or Inf, infundibulum; Bulge, HF-SC niche.

(B–D) Detection of Lrig1 protein (red) (B), Lrig1-EGFP (green) (C), and overlap (D) in telogen back skin.

(E) Detection of Lrig1 (red) and CD34 (green).

(F) Flow-cytometric analysis of Sca-1 expression in Lrig1-EGFP^{+ve} cells (green line) from telogen back skin. The black line indicates basal epidermal cells based on ItgA6 expression.

(G) Detection of Lrig1 (red) and Lgr5-EGFP (green) in anagen back skin. Is, isthmus; ORS, outer root sheath.

(H and I) Detection of Lrig1 (red) and Plet-1 (green) (H) and Lgr6-EGFP (green) (I) in telogen back skin. Arrows indicate Lgr6-EGFP expression in the IFE. The arrowhead indicates Lgr6-EGFP expression in the SG.

(J) Expression of Lrig1-EGFP (green) and Blimp1 (red) in the SG.

(K) qPCR analysis of marker expression in Lrig1-EGFP- and CD34-expressing cells.

Error bars represent the SEM (n = 4). Nuclei are counterstained with DAPI (blue). Scale bars represent 50 μm. See also Figure S1.

cells show altered expression of genes regulating growth when compared to basal IFE cells (Table S3). This suggests that there is a difference in their basic behavior in vivo that may reflect tissue-specific requirements for replenishment. In support, we observe a large number of Ki67^{+ve} cells in the Lrig1-expressing compartment, and during a short pulse with bromodeoxyuridine (BrdU), a much higher proportion of Lrig1-EGFP^{+ve} cells incorporate the label, when compared to both CD34^{+ve} HF–SCs and IFE cells (Figures 2F and 2G). The highly proliferative nature of Lrig1-expressing cells is strikingly similar to the behavior of Lrig1^{+ve} cells in the small intestine (Wong et al., 2012). Interestingly, unlike HF-SCs, epidermal Lrig1-EGFP^{+ve} cells show significant transcriptional overlap with Lrig1^{+ve} cells from the small intestine, which might underpin certain behavioral similarities (Figure S1H). We conclude that the upper pilosebaceous unit contains a distinct population of cells marked by Lrig1, which, based on their expression profile and incorporation of nucleoside analogue, represents one of the most proliferative cell compartments in telogen back skin.

Lrig1-Expressing Cells Maintain the Infundibulum and SGs as Independent Compartments

Based on the highly proliferative phenotype of Lrig1^{+ve} cells, we hypothesize that these cells play an active role in tissue maintenance. In order to address the behavior of these cells in vivo, Lrig1 KI mice were crossed with Rosa26-lsl-tdTomato mice, and Lrig1^{+ve} cells were labeled genetically with tdTomato during the resting phase of the hair cycle with a single administration of tamoxifen. Without the administration of tamoxifen, we do not detect tdTomato^{+ve} cells (Figure S2G). Analysis of back-skin samples taken 3 days after labeling revealed that the majority of tdTomato^{+ve} cells are found either as single cells or as two

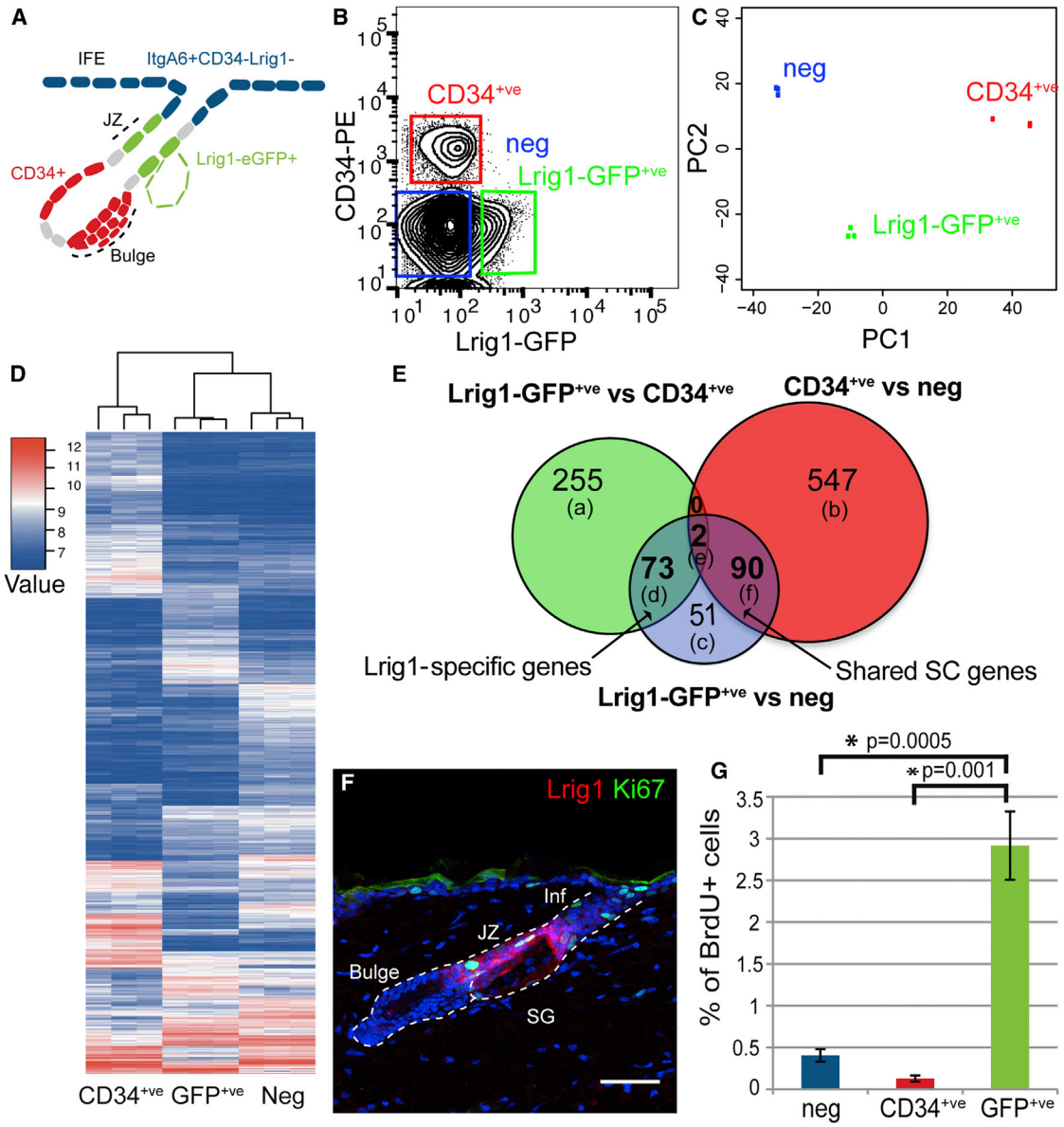

Figure 2. Lrig1 Marks a Unique and Highly Proliferative Compartment in the Epidermis

(A) Schematic diagram of isolated cell populations. Bulge, HF-SC niche.

(B) Isolation of ItgA6^{+ve}Lrig1-EGFP^{+ve}CD34^{-ve} (Lrig1-EGFP^{+ve}, green) ItgA6^{+ve}Lrig1-EGFP^{-ve}CD34^{+ve} (CD34^{+ve}, red) and ItgA6^{+ve}Lrig1-EGFP^{-ve}CD34^{-ve} (neg, blue) cells by flow cytometry.

(C) Principal component analysis of gene-expression profiles associated with Lrig1-EGFP^{+ve}, CD34^{+ve}, and negative cells.

(D and E) Heat map with the associated hierarchal clustering (D) and Venn diagram (E) of the upregulated probe sets associated with CD34^{+ve}, Lrig1-GFP^{+ve}, and negative epidermal cells. The number of individual probe sets in individual segments are indicated, and the associated probe sets are listed in Table S3 under (a)–(f). The (d) segment denotes genes enriched in Lrig1-EGFP^{+ve} cells, and the (f) segment denotes genes shared by Lrig1-EGFP^{+ve} and CD34^{+ve} cells.

(F) Detection of Ki67 (green) and Lrig1 (red) in telogen back skin. Nuclei are counterstained with DAPI (blue). Scale bars represent 50 μm.

(G) Quantification of BrdU incorporation after a 1 hr chase by flow cytometry.

Error bars represent the SEM (n = 4). See also Tables S1, S2, and S3.

cells in the JZ (Figures 3A and 3B). Less frequently, labeled cells are also seen in the SG, and rarely in the lower HF (Figure 3B). Over time, labeled progeny from the JZ expand upward to fill the entire infundibulum, where they persist for at least 1 year without migration into the IFE (Figures 3C–3G). Based on the long-term maintenance and expansion of labeled clones, we conclude that the infundibulum is maintained as an independent compartment by Lrig1-expressing SCs. Although the tail is asynchronous in its hair cycle, the observations from back skin are reiterated here (Figures S2H–S2L).

Approximately 20% of the labeling events were initially observed within the basal layer of the SG. This proportion remains

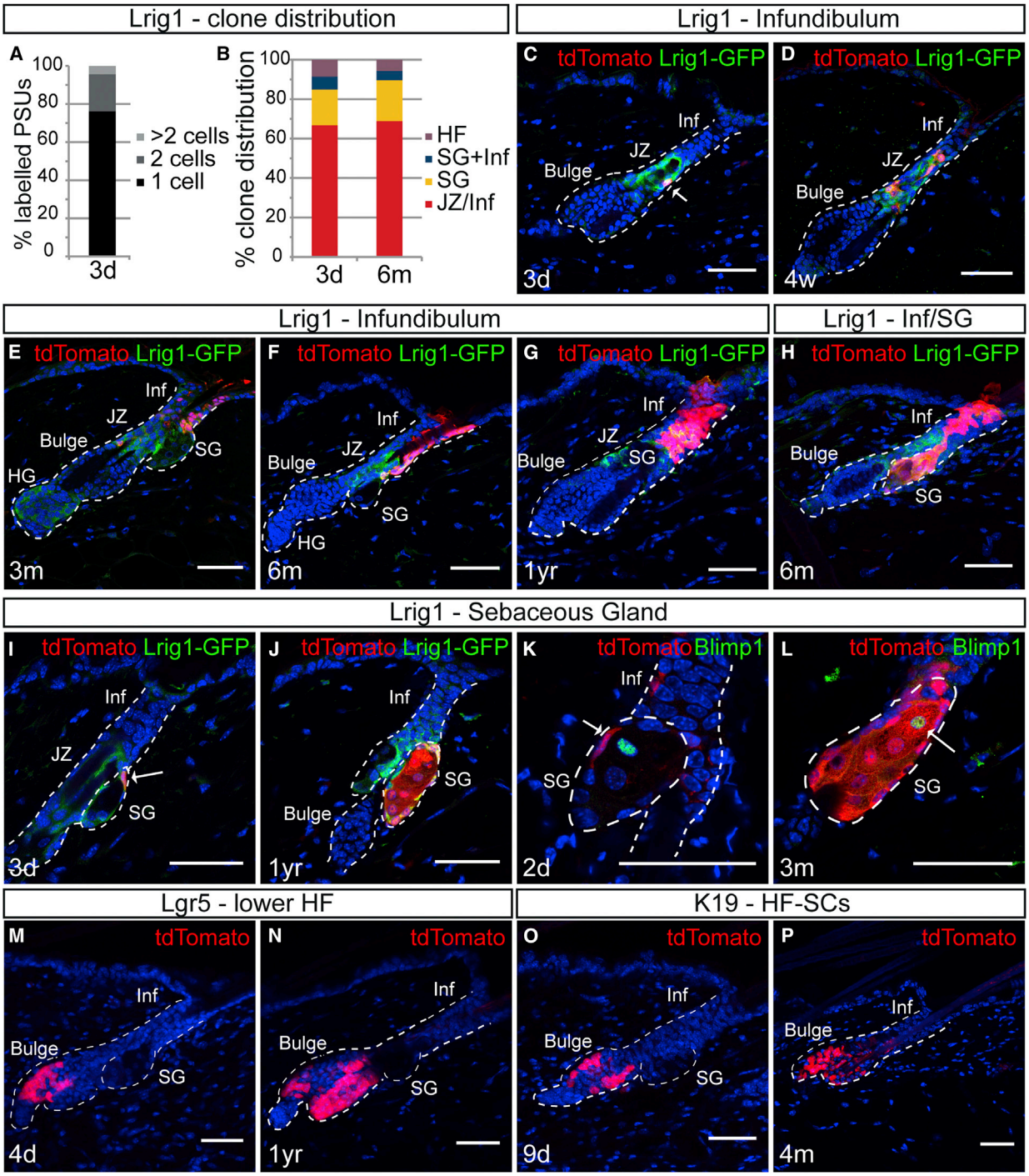

Figure 3. The Epidermis Is Maintained in Discrete Compartments

(A) Quantification of the proportion of labeled pilosebaceous units containing 1, 2, or >2 labeled cells 3 days (3d) post labeling. n = 100 pilosebaceous units (PSUs) from three mice.

(B) Quantification of clone distribution at 3 days and 6 months (6m) post labeling. n = 100 pilosebaceous units from three mice.

(C–J) Detection of tdTomato (red) and Lrig1-EGFP (green) after initiation of lineage tracing from Lrig1-expressing cells. Note the expansion of labeled progeny from Lrig1^{+ve} cells into the infundibulum and in SG over time and that labeled cells do not contribute to the IFE (C–H). HG, hair germ.

(K and L) Detection of tdTomato-labeled progeny of Lrig1-expressing cells and Blimp1 2 days and 3 months after labeling. Arrows indicate (K) initially labeled cells and (L) Blimp1^{+ve} progeny.

(M–P) Detection of tdTomato (red) after initiation of lineage tracing from Lgr5 (M and N) or K19 (O and P)-driven cre strains. Note that progeny of Lgr5^{+ve} and K19^{+ve} cells are restricted to the lower pilosebaceous unit.

Nuclei are counterstained with DAPI (blue). Scale bars represent 50 μm. See also Figure S2.

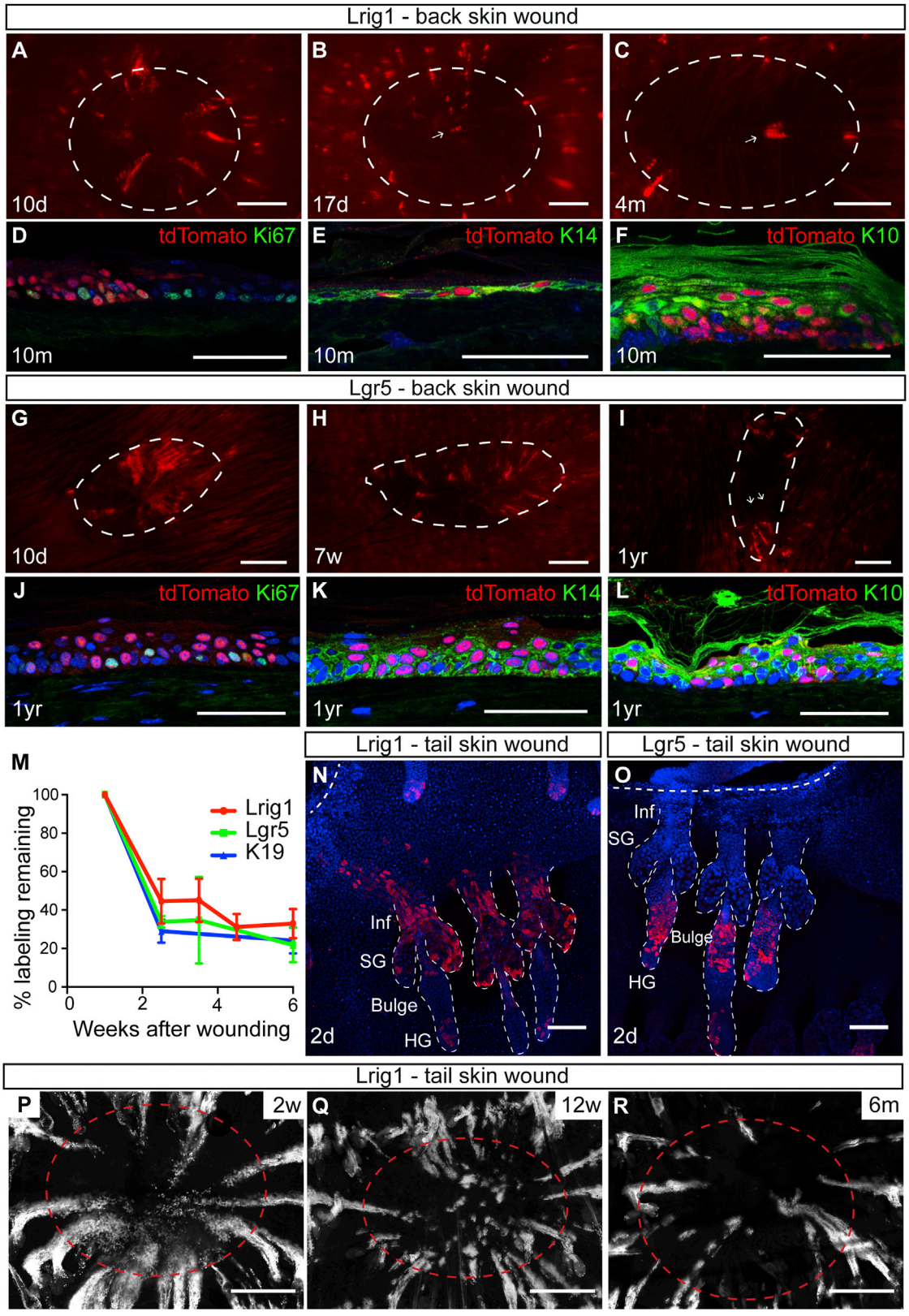

(legend on next page)

constant over time, indicating that resident cells in the SG are capable of long-term maintenance of this compartment (Figures 3B, 3I, and 3J). Initially, labeled Lrig1^{+ve} cells were negative for the marker Blimp1; however, over time tdTomato-labeled Lrig1 progeny became Blimp1^{+ve}, supporting the notion that Blimp1 marks terminally differentiated sebocytes (Figures 3K and 3L; Cottle et al., 2013). Given that ~30% of follicles have more than one labeled cell and less than 5% of pilosebaceous units have labeling in both the SG and infundibulum 6 months after labeling, we conclude that Lrig1^{+ve} cells at the single-cell level contribute only to the infundibulum or the SG (Figures 3A, 3B, and 3H).

The Epidermis Is Maintained in Discrete Compartments during Homeostasis

HF-SCs have previously been proposed as the master SC population at the top of a cellular hierarchy (Petersson et al., 2011). In order to assess the autonomy of epidermal compartmentalization, we investigated the relationship between the upper and lower pilosebaceous compartments. Our fate-mapping data from the ½ year and 1 year time points from Lrig1^{+ve} cells demonstrate that labeled cells are confined to the pilosebaceous unit and make no contribution to the IFE (Figures 3A–3L; Figures S2I–S2L). As the fraction of labeled clones in the lower part of the pilosebaceous unit is reduced over time, this strongly suggests that cells from the isthmus do not contribute to HF maintenance (Figure 3B). In order to determine whether HF-SCs repopulate the upper pilosebaceous compartment, as has been suggested for K15-expressing cells (Morris et al., 2004; Petersson et al., 2011), we utilize lineage tracing from the Lgr5-EGFP-ires-CreERT2 and K19CreER mouse models to specifically mark the HF-SC compartment. As previously reported, labeled cells are confined to this compartment at time points up to 1 year (Figures 3M–3P; Figure S2; Jaks et al., 2008; Youssef et al., 2010). This demonstrates that the upper and lower compartments of the pilosebaceous unit, as well as the IFE, are maintained in autonomous manners.

Tissue Regeneration Perturbs Homeostatic Compartmentalization

IFE SCs have been shown to be the major contributor to tissue regeneration following injury (Mascré et al., 2012); however, evidence from hairless mice and lineage tracing from pilosebaceous SCs supports a role for these cells in the regenerative response (Brownell et al., 2011; Ito et al., 2005; Langton et al., 2008; Snippert et al., 2010). It has also not been clear to what extent cells were specifically retained in the IFE following tissue repair based on their ancestry (Plikus et al., 2012). This is pertinent when considering the plasticity of SCs in vivo. In order to address the role of different defined cellular compartments in tissue regeneration, we investigated the behavior of tdTomato-labeled Lrig1^{+ve} and HF-SCs following skin wounding using serial imaging of live anaesthetized animals. One to two weeks after wounding, labeled cells from both pilosebaceous SC compartments were detected in a radial pattern in the wound area (Figures 4A–4C and 4G–4I; Figures S3A–S3C). Progeny are subsequently retained up to 1 year in the IFE (Figures 4D–4F and 4J–4L). This imaging technique allows quantitative analysis of labeled cells during the repair process in individual mice. This reveals a substantial reduction in the proportion of labeled cells 3 weeks after wounding (Figure 4M), which corresponds to the reduction in hyperplasia of the newly regenerated epidermis (Figures S3D and S3E). The reduction in labeled cells following 3 weeks is reminiscent of reported observations for progeny of keratin-15-expressing HF-SCs (Ito et al., 2005). We conclude that cells adopt IFE fate following injury irrespective of their ancestry.

Previous studies have focused on the tail epidermis, which facilitates high-resolution imaging. In order to investigate early events and whether there are significant differences between back and tail skin, we analyze three-dimensional (3D) reconstructions of epidermal-tail whole mounts. Two days following tail wounding, progeny of Lrig1^{+ve} cells appear at the wound margin more than 200 μm from the originating pilosebaceous unit (Figure 4N; Figure S3F). Analysis of HF-SCs shows delayed recruitment, given that labeled cells at day 2 were still retained in the lower pilosebaceous unit (Figure 4O; Figure S3F). Although the role of pilosebaceous SCs in tissue repair of the tail epidermis has been disputed (Mascré et al., 2012), we show here that they contribute to tissue repair irrespective of the population of origin (Figures 4P–4R; Figures S3G–S3I). This demonstrates that regional differences dictate whether cells are primed for an early or late regenerative response but do not impact their lineage plasticity in vivo.

Wounding, Not Mobilization, Drives Tumor Formation after K-Ras Activation

Recent evidence from studies of HF-SCs and their progeny implies that oncogenic responses upon K-Ras activation depend on the proliferation status and SC potential (White et al., 2011). In order to probe the response from highly proliferative Lrig1-expressing cells upon oncogenic stimulation, we utilized a Cre-inducible model for constitutive activation of K-Ras (Tuveson et al., 2004). Expression of K-Ras (G12D) causes increased phosphorylation of the downstream Erk kinase in the upper pilosebaceous unit and SG hyperplasia (Figures S4A–S4I). In line with the increased levels of Erk activation, there were significant changes to the structure and proliferation within the

Figure 4. Pilosebaceous SCs Break Compartment Boundaries in Response to Wounding and Convert to an IFE Fate

(A–C and G–I) Serial fluorescence imaging of tdTomato-labeled progeny of Lrig1^{+ve} (A–C) and Lgr5^{+ve} (G–I) cells in the reepithelized wound (red).

(D–F and J–L) Immunostaining of progeny of Lrig1^{+ve} (D–F) or Lgr5^{+ve} (J–L) cells in the regenerated IFE 10 months or 1 year after wounding.

(M) Quantification of labeling after wounding of Lrig1, Lgr5, and K19 CreER mice by serial fluorescence imaging normalized to area of wound labeled 10 days after wounding. Error bars represent the SEM (Lgr5, n = 4; K19, n = 3; Lrig1, n = 5 mice).

(N and O) Progeny of Lrig1^{+ve} (N) and Lgr5^{+ve} (O) cells (red) at day 2 following tail wounding (distance quantified in Figure S3F).

(P–R) Progeny of Lrig1^{+ve} cells detected in whole mounts of tail wound epidermis. The demarcated lines depict the wound margin.

Nuclei are counterstained with DAPI (blue). Scale bars represent 1 mm (A–C and G–I), 50 μm (D–F and J–L), 100 μm (N and O), and 500 μm (P–R). See also Figure S3.

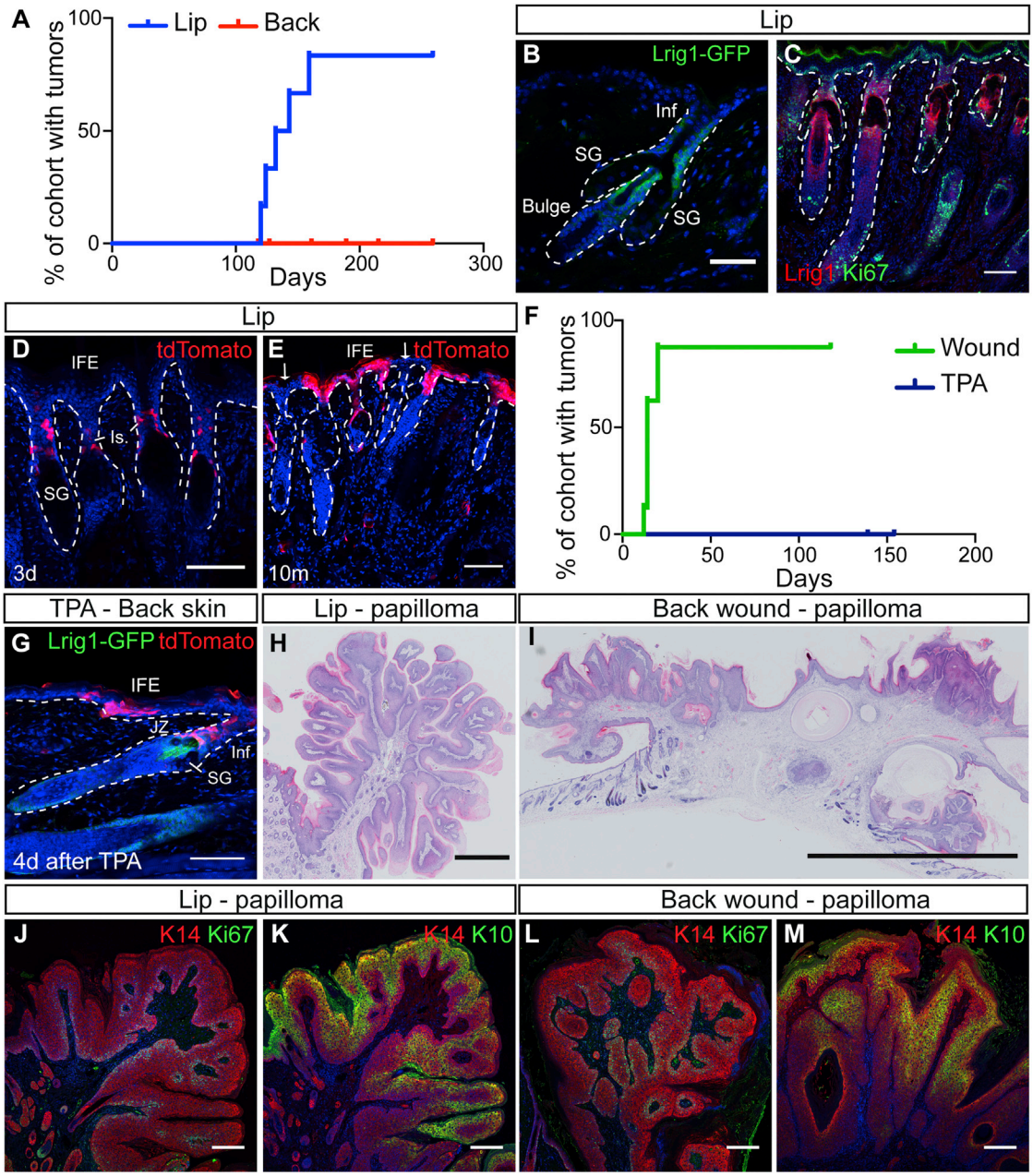

Figure 5. Wounding Induces K-Ras-Driven Papillomas

(A) Spontaneous papilloma development in Lrig1 KI/LSL-K-Ras (G12D) mice (lip, n = 6; back, n = 8).

(B) Lrig1-EGFP (green) detected in lip epidermis.

(C) Detection of Lrig1 (red) and Ki67 (green) in lip epidermis.

(D and E) Progeny of Lrig1^{+ve} cells (red) detected in lip epidermis after short and long chase. Arrows indicate absence of labeling in the IFE adjacent to unlabeled infundibula.

(F) TPA- and wound-induced papilloma development in Lrig1 KI/LSL-K-Ras (G12D) mice (TPA, n = 5; wound, n = 8).

(G–M) Detection of tdTomato-labeled progeny of Lrig1-expressing cells in the IFE 4 days after the final TPA treatment of Lrig1 KI/LSL tdTomato mice. Hematoxylin and eosin (H&E) stain of lip papilloma (H) and (I) wound-induced papilloma on the back. Detection of Ki67 (green) and keratin 10 (green) in papillomas on the lip (J and K) and back (L and M) counterstained with keratin 14 (red) and DAPI (blue).

Scale bars represent 50 μm (B and G), 100 μm (C–E), 1 mm (H), 5 mm (I), and 200 μm (J–M). See also Figure S4.

infundibulum, but we observed no tumor development and very little effect to the IFE on back skin (Figures S4A–S4E and S4G–S4I). Mice subsequently developed benign papillomas in lip epidermis from 4 months following the induction of K-Ras (G12D), as described for other cre drivers (Figure 5A; Lapouge et al., 2011; van der Weyden et al., 2011).

In order to understand the difference in epidermal-tumor susceptibility between the two sites, we analyzed Lrig1 expression and cell behavior in lip epithelium. SG hyperplasia was also evident in the lip epidermis after K-Ras activation (Figure S4F). As in back skin, Lrig1 expression was detected in highly proliferative cells in the pilosebaceous unit and never in the IFE (Figures 5B and 5C). Similarly, fate mapping showed that labeled cells were initially found in the upper isthmus; however, at later time points, tdTomato^{+ve} cells were detected in the IFE, and always in association with fully labeled infundibula (Figures 5D and 5E). This is reminiscent of the behavior of Lrig1-expressing cells upon wounding. Basal cell carcinomas, which are driven by aberrant Shh signaling, only form from cells in the IFE (Youssef et al., 2010; Kasper et al., 2011; Wong and Reiter, 2011). In order to test whether mobilization of SCs from the pilosebaceous unit is sufficient for tumor induction, mice expressing the oncogenic K-Ras mutation in Lrig1-expressing cells were treated with the tumor promoter 12-O-tetradecanoylphorbol-13-acetate (TPA). TPA induces a robust inflammatory response, which stimulates migration of Lrig1-expressing cells into the IFE (Figure 5G). However, this is not sufficient to induce tumor formation (Figure 5F). Instead, a more abrasive approach was adopted wherein the oncogenic mutation was combined with full-thickness wounding. This drives very rapid and efficient papilloma formation in back skin from the Lrig1^{+ve} compartment (Figure 5F). The tumors are similar to those forming from the lips and display a high number of proliferating cells, as well as a differentiated compartment (Figures 5H–5M). We conclude that oncogenic mutations in SCs perturb normal behavior within the tissue, and that wounding in addition to simple migration out of the natural compartment is required for tumor initiation.

DISCUSSION

In this study we define the cellular networks that underlie epidermal homeostasis as founded in the existence of subsets of SCs with distinct tissue contributions. Here, the lower part of the pilosebaceous unit, the infundibulum, the SG, and the IFE are maintained as independent compartments. The normal boundaries are broken upon wounding, and cells are rapidly recruited into the wounded region, where they subsequently contribute long term to tissue homeostasis, irrespective of their ancestry. Wounding is also the auxiliary signal required for inducing tumor formation from Lrig1-positive SCs expressing oncogenic K-Ras.

The upper pilosebaceous unit contains multiple overlapping populations of SCs; however, it has been difficult to rectify differing observations between expression studies, lineage-tracing studies, and reporter models (Horsley et al., 2006; Levy et al., 2005; Snippert et al., 2010; Brownell et al., 2011). Careful examination of individual markers has enabled us to dissect this relationship. Here, we show that Plet1/MTS24 and Lrig1 are both expressed in the upper isthmus. Lrig1-expressing SCs in the SG will renew Blimp1^{+ve} sebocytes over time. The expression of Lgr6 in multiple compartments makes fate mapping from Lgr6-expressing cells very difficult to interpret, because labeled progeny might arise from Lgr6^{+ve} cells in the different structures rather than from a single source as previously suggested (Blanpain, 2010). A much simpler model for tissue homeostasis is consequently emerging, wherein during homeostasis, SCs only contribute to their resident compartment.

Lineage-specific amplification by defined SC populations is beginning to emerge as a general mechanism for tissue replenishment (Van Keymeulen and Blanpain, 2012). The best examples are the mammary gland and prostate, wherein the luminal and myoepithelial compartments are maintained independently throughout life (Van Keymeulen et al., 2011; Ousset et al., 2012; Choi et al., 2012). We demonstrate that the different functional components of the epidermis are maintained in a similar manner during steady-state homeostasis, and we propose that this represents a general mechanism for the maintenance of complex cellular systems. This enables the tissue to respond to specific requirements of individual regions. In this manner, the epidermis can simultaneously cater to the requirements for cyclic growth of the HF and the constant maintenance of the SG and IFE. Our study identifies Lrig1-expressing cells in the upper isthmus as a highly proliferative SC population responsible for maintenance of the infundibulum. One major feature of the infundibulum is the mechanical stress exerted from the hair shaft as it protrudes out through the skin. In agreement with the increased stress levels, we do observe expression of proinflammatory cytokines such as *Ccl2* and *Ccl7* specifically in Lrig1^{+ve} cells. By having a dedicated compartment of stem cells, it is possible to specifically respond to the requirement of the infundibulum for constant repair.

Lrig1 has been characterized as a negative regulator of proliferation both in vivo and in vitro (Gur et al., 2004; Jensen et al., 2009; Laederich et al., 2004; Wong et al., 2012). The proliferative behavior of Lrig1-expressing stem cells in vivo is, however, analogous to their counterparts in the small intestine, where Lrig1 controls SC proliferation by modulating the amplitude of ErbB signaling (Wong et al., 2012). In both cases the inductive signals for proliferation must either overcome its inhibitory effects or utilize pathways that are not regulated by Lrig1. Future analysis of the genes identified as differentially expressed in Lrig1^{+ve} cells is likely to shed light on gene networks responsible for the unique behavior of these cells.

An important function of SCs in adult tissues is to contribute to wound repair following injury (Plikus et al., 2012). A major difference between SCs and more committed progeny within the epidermis is the ability of SCs to be retained once the tissue is healed (Mascré et al., 2012). Tissue contribution after injury is consequently a measure for SC potential. IFE-derived stem cells were recently shown to be the predominant contributor to tissue repair (Mascré et al., 2012); however, evidence from hairless mice and the long-term retention of cells from the pilosebaceous unit suggest that these cells are likewise involved (Langton et al., 2008; Ito et al., 2005; Levy et al., 2007; Brownell et al., 2011). The observation that cells can move across boundaries upon wounding shows that cells are not lineage restricted, but that the microenvironment, rather than cellular ancestry, dictates cell behavior in vivo. Moreover, the apparently proportional retention of all pilosebaceous SC progenies supports the notion that this is a stochastic rather than a hard-wired process.

Experimental evidence demonstrates that epidermal SCs have the potential to initiate tumor formation (Lapouge et al., 2011; White et al., 2011); however, tumors formed upon expression of oncogenic K-Ras are generally associated with areas of

abrasion (van der Weyden et al., 2011). We observe that expression of K-Ras G12D in Lrig1-expressing cells drives SG and infundibula hyperplasia without affecting the IFE significantly. The speed and the reproducibility with which these tumors form following wounding strongly suggest that additional mutations are not required. We expect that in the future this model will provide an attractive platform for the identification of genes involved in tumor formation. It is evident that loss of p53 combined with K-Ras activation drives malignant progression (Caulin et al., 2007; Lapouge et al., 2011; White et al., 2011), and it is very probable that such combinations will not need additional wound-associated signals to initiate tumor formation from Lrig1-expressing cells.

In summary, we have identified Lrig1 as a marker of the SC compartment responsible for independent maintenance of the infundibulum and SG. A picture is now emerging in which the epidermis is compartmentalized during homeostasis, and this provides a functional explanation for the SC heterogeneity in the pilosebaceous unit. We predict that it will be possible to observe similar compartmentalized patterns in other complex organs. This is potentially a general method for controlling tissue homeostasis, in that it provides a simple solution to cater for regional differences in the requirement for tissue replenishment.

EXPERIMENTAL PROCEDURES

Mice

Lrig1-EGFP-ires-CreERT2 mice were generated by knocking an EGFP-ires-CreERT2 cassette into the endogenous Lrig1 locus in C57Bl6 embryonic stem cells. Lgr5-EGFP-ires-CreERT2, K19CreER, K-Ras-lsl-G12D, and Rosa-lsl-tdTomato mice have been described previously (Barker et al., 2007; Madisen et al., 2010; Means et al., 2008; Tuveson et al., 2004). DNA labeling was achieved by single intraperitoneal (i.p.) injections of 1 mg BrdU. For lineage analysis, mice received single i.p. injections of tamoxifen dissolved in corn oil (Lrig1, 100 μg; Lgr5/KI9, 3 mg). Activation of K-Ras was achieved by topical application of 100 μg 4-hydroxytamoxifen in acetone. Wound biopsies were carried out with a circular biopsy punch on the dorsal (5 mm) or tail (2 mm) skin. For TPA treatment, 1 μg of TPA in acetone was applied topically to back skin on days 1, 4, 8, and 11. Serial imaging was performed on anaesthetized mice using a Leica M165FC dissecting microscope. All in vivo experiments were performed under the terms of a UK Home Office license.

Immunohistochemistry and Immunofluorescence

Immunohistochemistry was performed using the ImmPRESS polymer detection kit (Vector Labs). For immunofluorescence staining, samples were blocked in 0.5% BSA, 0.5% fish skin gelatin, and 0.1% Triton X-100 before overnight incubation in primary antibody as listed in Table S4. Primary antibodies were detected with appropriate Alexa-fluorophore-conjugated secondary donkey antibodies (Invitrogen). Whole mounts of tail epidermis, tissue preparation, and images were acquired as described previously (Jensen et al., 2009).

Isolation of Cells for Flow Cytometry

Keratinocytes were isolated and sorted from mouse back skin as previously described (Jensen et al., 2010). Hematopoietic and endothelial cells were excluded by negative selection of $CD45^{+ve}$ and $CD31^{+ve}$ cells. Flow cytometry was carried out using a CyAN ADP (Beckman Coulter) and an LSRFortessa (BD Biosciences) flow cytometer, and cell sorting was carried out on a FACSAria (BD Biosciences) and a MoFlo Legacy cell sorter (Beckman Coulter). An APC BrdU Flow Kit (BD Pharmingen) was used to assess BrdU incorporation. Data were analyzed using FlowJo software.

RNA Extraction and Quantitative PCR

Total RNA was isolated from flow-sorted cells using the PureLink RNA Micro Kit with on-column DNase digestion (Invitrogen). Complementary DNA was synthesized and analyzed by quantitative PCR (qPCR) as described previously (Wong et al., 2012). For global gene-expression profiling, RNA was pre-amplified (Ovation RNA Amplification System, NuGEN) and hybridized to MouseWG-6 v.2 BeadChips (Illumina).

Microarray Analysis

Raw data from the MouseWG-6 v.2 BeadChips were processed using the R package "lumi" (Du et al., 2008). A variance-stabilizing transformation, quantile normalization, and quality control were performed on the expression data. Nonexpressed probes (detection p value ≥ 0.01 in all samples) were removed from downstream analysis. To test for differential expression, the R package LIMMA was used (Smyth, 2004). Multiple testing correction on all probes and across contrasts was performed by controlling the false discovery rate. The "nestedF" strategy was used to adjust the F statistic p values to find probes that were differentially expressed in at least one sample. Probes were considered significant if the adjusted p value was ≤ 0.05 and the log fold change was ≥ 0.5.

For gene-set enrichment analysis, expressed probes were ranked according to their association with Lrig1-GFP^{+ve} and -GFP^{-ve} cells in the small intestine. Identified gene signatures associated with epidermal SCs were subsequently analyzed for their association with Lrig1-GFP^{+ve} or -GFP^{-ve} cells in the intestine (http://www.broadinstitute.org/gsea/index.jsp; Mootha et al., 2003). GO analysis for biological processes was carried out on differentially expressed gene sets using the DAVID bioinformatics resource (Huang et al., 2009).

ACCESSION NUMBERS

The European Bioinformatics Institute ArrayExpress accession numbers for data reported in this paper are E-MTAB-1602 and E-MTAB-1606.

SUPPLEMENTAL INFORMATION

Supplemental Information includes four figures and four tables and can be found with this article online at http://dx.doi.org/10.1016/j.stem.2013.07.010.

ACKNOWLEDGMENTS

We thank Fiona Watt for assistance in generating the Lrig1 KI mouse model; Tyler Jacks and Guoqiang Gu for making their mouse models available; the Cambridge Stem Cell Institute core facilities and the Cambridge Genomics Services for technical assistance; Michaela Frye for excellent suggestions; and Austin Smith, Kristian Helin, and members of the Jensen laboratory for comments on the manuscript. We acknowledge Ferda Oeztuerk-Winder and Juan Jose Ventura for tissue from the Lgr6 mouse, and Clare Blackburn for the Plet1 antibody. This work was supported by the UK Medical Research Council (MRC), the Wellcome Trust, the Lundbeck Foundation, and the Danish Medical Research Council. K.J. is a Wellcome Trust Career Development fellow (WT088454MA). M.E.P. and F.N. are funded by an MRC PhD studentship and a Yousef Jameel Scholarship, respectively. M.E.P. and K.B.J. conceived and designed the study, performed experiments, analyzed the data, and wrote the manuscript. P.L., F.N., and B.G. performed the bioinformatics analysis of the microarray data. All authors commented on the manuscript. K.B.J. supervised the project.

Received: April 7, 2013
Revised: June 18, 2013
Accepted: July 16, 2013
Published: August 15, 2013

REFERENCES

Alcolea, M.P., and Jones, P.H. (2013). Tracking cells in their native habitat: lineage tracing in epithelial neoplasia. Nat. Rev. Cancer *13*, 161–171.

Barker, N., van Es, J.H., Kuipers, J., Kujala, P., van den Born, M., Cozijnsen, M., Haegebarth, A., Korving, J., Begthel, H., Peters, P.J., and Clevers, H. (2007). Identification of stem cells in small intestine and colon by marker gene Lgr5. Nature *449*, 1003–1007.

Barker, N., van Oudenaarden, A., and Clevers, H. (2012). Identifying the stem cell of the intestinal crypt: strategies and pitfalls. Cell Stem Cell *11*, 452–460.

Blanpain, C. (2010). Stem cells: Skin regeneration and repair. Nature *464*, 686–687.

Brownell, I., Guevara, E., Bai, C.B., Loomis, C.A., and Joyner, A.L. (2011). Nerve-derived sonic hedgehog defines a niche for hair follicle stem cells capable of becoming epidermal stem cells. Cell Stem Cell *8*, 552–565.

Caulin, C., Nguyen, T., Lang, G.A., Goepfert, T.M., Brinkley, B.R., Cai, W.W., Lozano, G., and Roop, D.R. (2007). An inducible mouse model for skin cancer reveals distinct roles for gain- and loss-of-function p53 mutations. J. Clin. Invest. *117*, 1893–1901.

Choi, N., Zhang, B., Zhang, L., Ittmann, M., and Xin, L. (2012). Adult murine prostate basal and luminal cells are self-sustained lineages that can both serve as targets for prostate cancer initiation. Cancer Cell *21*, 253–265.

Clayton, E., Doupé, D.P., Klein, A.M., Winton, D.J., Simons, B.D., and Jones, P.H. (2007). A single type of progenitor cell maintains normal epidermis. Nature *446*, 185–189.

Cottle, D.L., Kretzschmar, K., Schweiger, P.J., Quist, S.R., Gollnick, H.P., Natsuga, K., Aoyagi, S., and Watt, F.M. (2013). c-MYC-induced sebaceous gland differentiation is controlled by an androgen receptor/p53 axis. Cell Rep *3*, 427–441.

Du, P., Kibbe, W.A., and Lin, S.M. (2008). lumi: a pipeline for processing Illumina microarray. Bioinformatics *24*, 1547–1548.

Frances, D., and Niemann, C. (2012). Stem cell dynamics in sebaceous gland morphogenesis in mouse skin. Dev. Biol. *363*, 138–146.

Ghazizadeh, S., and Taichman, L.B. (2001). Multiple classes of stem cells in cutaneous epithelium: a lineage analysis of adult mouse skin. EMBO J. *20*, 1215–1222.

Gur, G., Rubin, C., Katz, M., Amit, I., Citri, A., Nilsson, J., Amariglio, N., Henriksson, R., Rechavi, G., Hedman, H., et al. (2004). LRIG1 restricts growth factor signaling by enhancing receptor ubiquitylation and degradation. EMBO J. *23*, 3270–3281.

Horsley, V., O'Carroll, D., Tooze, R., Ohinata, Y., Saitou, M., Obukhanych, T., Nussenzweig, M., Tarakhovsky, A., and Fuchs, E. (2006). Blimp1 defines a progenitor population that governs cellular input to the sebaceous gland. Cell *126*, 597–609.

Huang, W., Sherman, B.T., and Lempicki, R.A. (2009). Systematic and integrative analysis of large gene lists using DAVID bioinformatics resources. Nat. Protoc. *4*, 44–57.

Ito, M., Liu, Y., Yang, Z., Nguyen, J., Liang, F., Morris, R.J., and Cotsarelis, G. (2005). Stem cells in the hair follicle bulge contribute to wound repair but not to homeostasis of the epidermis. Nat. Med. *11*, 1351–1354.

Jaks, V., Barker, N., Kasper, M., van Es, J.H., Snippert, H.J., Clevers, H., and Toftgård, R. (2008). Lgr5 marks cycling, yet long-lived, hair follicle stem cells. Nat. Genet. *40*, 1291–1299.

Jaks, V., Kasper, M., and Toftgård, R. (2010). The hair follicle-a stem cell zoo. Exp. Cell Res. *316*, 1422–1428.

Jensen, U.B., Yan, X., Triel, C., Woo, S.H., Christensen, R., and Owens, D.M. (2008). A distinct population of clonogenic and multipotent murine follicular keratinocytes residing in the upper isthmus. J. Cell Sci. *121*, 609–617.

Jensen, K.B., Collins, C.A., Nascimento, E., Tan, D.W., Frye, M., Itami, S., and Watt, F.M. (2009). Lrig1 expression defines a distinct multipotent stem cell population in mammalian epidermis. Cell Stem Cell *4*, 427–439.

Jensen, K.B., Driskell, R.R., and Watt, F.M. (2010). Assaying proliferation and differentiation capacity of stem cells using disaggregated adult mouse epidermis. Nat. Protoc. *5*, 898–911.

Kasper, M., Jaks, V., Are, A., Bergström, A., Schwäger, A., Svärd, J., Teglund, S., Barker, N., and Toftgård, R. (2011). Wounding enhances epidermal tumorigenesis by recruiting hair follicle keratinocytes. Proc. Natl. Acad. Sci. USA *108*, 4099–4104.

Laederich, M.B., Funes-Duran, M., Yen, L., Ingalla, E., Wu, X., Carraway, K.L., 3rd, and Sweeney, C. (2004). The leucine-rich repeat protein LRIG1 is a negative regulator of ErbB family receptor tyrosine kinases. J. Biol. Chem. *279*, 47050–47056.

Langton, A.K., Herrick, S.E., and Headon, D.J. (2008). An extended epidermal response heals cutaneous wounds in the absence of a hair follicle stem cell contribution. J. Invest. Dermatol. *128*, 1311–1318.

Lapouge, G., Youssef, K.K., Vokaer, B., Achouri, Y., Michaux, C., Sotiropoulou, P.A., and Blanpain, C. (2011). Identifying the cellular origin of squamous skin tumors. Proc. Natl. Acad. Sci. USA *108*, 7431–7436.

Levy, V., Lindon, C., Harfe, B.D., and Morgan, B.A. (2005). Distinct stem cell populations regenerate the follicle and interfollicular epidermis. Dev. Cell *9*, 855–861.

Levy, V., Lindon, C., Zheng, Y., Harfe, B.D., and Morgan, B.A. (2007). Epidermal stem cells arise from the hair follicle after wounding. FASEB J. *21*, 1358–1366.

Lu, L., Teixeira, V.H., Yuan, Z., Graham, T.A., Endesfelder, D., Kolluri, K., Al-Juffali, N., Hamilton, N., Nicholson, A.G., Falzon, M., et al. (2013). LRIG1 regulates cadherin-dependent contact inhibition directing epithelial homeostasis and pre-invasive squamous cell carcinoma development. J. Pathol. *229*, 608–620.

Madisen, L., Zwingman, T.A., Sunkin, S.M., Oh, S.W., Zariwala, H.A., Gu, H., Ng, L.L., Palmiter, R.D., Hawrylycz, M.J., Jones, A.R., et al. (2010). A robust and high-throughput Cre reporting and characterization system for the whole mouse brain. Nat. Neurosci. *13*, 133–140.

Mascré, G., Dekoninck, S., Drogat, B., Youssef, K.K., Broheé, S., Sotiropoulou, P.A., Simons, B.D., and Blanpain, C. (2012). Distinct contribution of stem and progenitor cells to epidermal maintenance. Nature *489*, 257–262.

Means, A.L., Xu, Y., Zhao, A., Ray, K.C., and Gu, G. (2008). A CK19(CreERT) knockin mouse line allows for conditional DNA recombination in epithelial cells in multiple endodermal organs. Genesis *46*, 318–323.

Morris, R.J., Liu, Y., Marles, L., Yang, Z., Trempus, C., Li, S., Lin, J.S., Sawicki, J.A., and Cotsarelis, G. (2004). Capturing and profiling adult hair follicle stem cells. Nat. Biotechnol. *22*, 411–417.

Mootha, V.K., Lindgren, C.M., Eriksson, K.F., Subramanian, A., Sihag, S., Lehar, J., Puigserver, P., Carlsson, E., Ridderstråle, M., Laurila, E., et al. (2003). PGC-1alpha-responsive genes involved in oxidative phosphorylation are coordinately downregulated in human diabetes. Nat. Genet. *34*, 267–273.

Nagao, K., Kobayashi, T., Moro, K., Ohyama, M., Adachi, T., Kitashima, D.Y., Ueha, S., Horiuchi, K., Tanizaki, H., Kabashima, K., et al. (2012). Stress-induced production of chemokines by hair follicles regulates the trafficking of dendritic cells in skin. Nat. Immunol. *13*, 744–752.

Nijhof, J.G., Braun, K.M., Giangreco, A., van Pelt, C., Kawamoto, H., Boyd, R.L., Willemze, R., Mullenders, L.H., Watt, F.M., de Gruijl, F.R., and van Ewijk, W. (2006). The cell-surface marker MTS24 identifies a novel population of follicular keratinocytes with characteristics of progenitor cells. Development *133*, 3027–3037.

Nowak, J.A., Polak, L., Pasolli, H.A., and Fuchs, E. (2008). Hair follicle stem cells are specified and function in early skin morphogenesis. Cell Stem Cell *3*, 33–43.

Ousset, M., Van Keymeulen, A., Bouvencourt, G., Sharma, N., Achouri, Y., Simons, B.D., and Blanpain, C. (2012). Multipotent and unipotent progenitors contribute to prostate postnatal development. Nat. Cell Biol. *14*, 1131–1138.

Owens, D.M., and Watt, F.M. (2003). Contribution of stem cells and differentiated cells to epidermal tumours. Nat. Rev. Cancer *3*, 444–451.

Petersson, M., Brylka, H., Kraus, A., John, S., Rappl, G., Schettina, P., and Niemann, C. (2011). TCF/Lef1 activity controls establishment of diverse stem and progenitor cell compartments in mouse epidermis. EMBO J. *30*, 3004–3018.

Plikus, M.V., Gay, D.L., Treffeisen, E., Wang, A., Supapannachart, R.J., and Cotsarelis, G. (2012). Epithelial stem cells and implications for wound repair. Semin. Cell Dev. Biol. *23*, 946–953.

Rock, J.R., and Hogan, B.L. (2011). Epithelial progenitor cells in lung development, maintenance, repair, and disease. Annu. Rev. Cell Dev. Biol. *27*, 493–512.

Smyth, G.K. (2004). Linear models and empirical bayes methods for assessing differential expression in microarray experiments. Stat. Appl. Genet. Mol. Biol. *3*, Article3.

Snippert, H.J., Haegebarth, A., Kasper, M., Jaks, V., van Es, J.H., Barker, N., van de Wetering, M., van den Born, M., Begthel, H., Vries, R.G., et al. (2010). Lgr6 marks stem cells in the hair follicle that generate all cell lineages of the skin. Science *327*, 1385–1389.

Tuveson, D.A., Shaw, A.T., Willis, N.A., Silver, D.P., Jackson, E.L., Chang, S., Mercer, K.L., Grochow, R., Hock, H., Crowley, D., et al. (2004). Endogenous oncogenic K-ras(G12D) stimulates proliferation and widespread neoplastic and developmental defects. Cancer Cell *5*, 375–387.

van der Weyden, L., Alcolea, M.P., Jones, P.H., Rust, A.G., Arends, M.J., and Adams, D.J. (2011). Acute sensitivity of the oral mucosa to oncogenic K-ras. J. Pathol. *224*, 22–32.

Van Keymeulen, A., and Blanpain, C. (2012). Tracing epithelial stem cells during development, homeostasis, and repair. J. Cell Biol. *197*, 575–584.

Van Keymeulen, A., Rocha, A.S., Ousset, M., Beck, B., Bouvencourt, G., Rock, J., Sharma, N., Dekoninck, S., and Blanpain, C. (2011). Distinct stem cells contribute to mammary gland development and maintenance. Nature *479*, 189–193.

White, A.C., Tran, K., Khuu, J., Dang, C., Cui, Y., Binder, S.W., and Lowry, W.E. (2011). Defining the origins of Ras/p53-mediated squamous cell carcinoma. Proc. Natl. Acad. Sci. USA *108*, 7425–7430.

Wong, S.Y., and Reiter, J.F. (2011). Wounding mobilizes hair follicle stem cells to form tumors. Proc. Natl. Acad. Sci. USA *108*, 4093–4098.

Wong, V.W., Stange, D.E., Page, M.E., Buczacki, S., Wabik, A., Itami, S., van de Wetering, M., Poulsom, R., Wright, N.A., Trotter, M.W., et al. (2012). Lrig1 controls intestinal stem-cell homeostasis by negative regulation of ErbB signalling. Nat. Cell Biol. *14*, 401–408.

Youssef, K.K., Van Keymeulen, A., Lapouge, G., Beck, B., Michaux, C., Achouri, Y., Sotiropoulou, P.A., and Blanpain, C. (2010). Identification of the cell lineage at the origin of basal cell carcinoma. Nat. Cell Biol. *12*, 299–305.